Langmuir
Article
pubs.acs.org/Langmuir

Monodisperse Samarium and Cerium Orthovanadate Nanocrystals and Metal Oxidation States on the Nanocrystal Surface

Thanh-Dinh Nguyen, Cao-Thang Dinh, and Trong-On Do*

Department of Chemical Engineering, Laval University, Quebec G1K 7P4, Canada

Received April 19, 2009. Revised Manuscript Received May 31, 2009

A new solvothermal method has been developed for the synthesis of monodisperse $SmVO_4$ and $CeVO_4$ nanocrystals with controlled size and shape. The obtained materials were characterized by X-ray photoelectron spectroscopy (XPS), X-ray diffraction (XRD), transmission electron microscopy (TEM), and selected area electron diffraction (SAED) techniques. The results reveal that uniform nanocrystals and pure tetragonal phase of $SmVO_4$ and $CeVO_4$ can be achieved. To investigate the oxidation states of the metals on the mixed oxide nanocrystal surface, the XPS technique was employed. The results exhibit that only one oxidation state of samarium, cerium, and vanadium for each metal (e.g., Sm^{3+}, Ce^{3+}, V^{5+}) was surprisingly well stable on the particle surface at the nanoscale, even after calcination, while the existence of two oxidation states of these metals is observed (e.g., Sm^{3+}/Sm^{2+}, Ce^{4+}/Ce^{3+}, V^{5+}/V^{4+}) in the corresponding single metal oxide nanocrystals.

1. Introduction

Rare earth orthovanadate (Re−V−O) crystals have potential applications as catalysts and support owing to their high surface area, thermal stability, and oxygen storage/release capacity (OSC).[1−3] These materials have been used as oxygen ion conductors in solid oxide fuel cells, as three way catalysts (TWCs), and as high-activity catalysts in oxidative dehydrogenation of propane to propene and selective oxidation of hydrogen sulfide to elemental sulfur at low reaction temperatures.[4−7]

In recent years, the synthesis of these nanosized Re−V−O crystal systems with controlled size and shape has attracted much interest due their extensive potential applications in different fields, for example, optics, electrical, magnetic, and catalytic fields.[8,9] Their unique properties are due to not only their size-dependent properties but also the combination of the properties of individual components and of stoichiometry and symmetry in the mixed oxide crystals which are not available in single metal oxide nanocrystals (NCs).[10,11] Furthermore, the metal oxidation states in the mixed oxide NCs as well as the crystal structure are also considered to be responsible for their catalytic performance[12] and potential application.[13,14]

In order to better understand the metal oxidation states on the mixed oxide surface at the nanoscale, we have developed a novel, simple, and reproducible method for the synthesis of monodisperse $SmVO_4$ and $CeVO_4$ nanocrystals. In this work, we have focused on the synthesis of nanocubes and nanospheres. However, different shapes and sizes of these monodisperse mixed oxide NCs can be also obtained using this same approach. Although several methods have been reported,[15−18] however, to the best of our knowledge, up to date, few studies have been focused on the synthesis of uniform $SmVO_4$ and $CeVO_4$ nanospheres. Furthermore, our method is fundamentally different from the previous methods for the synthesis of these types of materials in aqueous[19,20] and organic[21,22] solutions. The monodisperse $SmVO_4$ and $CeVO_4$ NCs obtained by our approach are characterized by X-ray diffraction (XRD), transmission electron microscopy (TEM), and selected area electron diffraction (SAED). The oxidation states of the metals in the lattice are examined by X-ray photoelectron spectroscopy (XPS) both before and after calcination, compared to those of the corresponding single metal oxide NCs (e.g., Sm_2O_3, CeO_2, V_2O_5).

2. Experimental Section

Starting Materials. All chemicals were used as received without further purification. Samarium nitrate hexahydrate ($Sm(NO_3)_3 \cdot 6H_2O$, 99.9%), cerium nitrate hexahydrate ($Ce(NO_3)_3 \cdot 6H_2O$, 99.9%), vanadium pentaoxide (V_2O_5, 99.6%), tetraoctylammonium bromide ($[CH_3(CH_2)_7]_4NBr$ or TOABr, ≥98%), potassium oleate ($C_{17}H_{34}COOK$ or KOA, 40 wt % paste in water), and oleylamine ($C_{18}H_{35}NH_2$ or OM, tech. grade, 70%)

*To whom correspondence should be addressed. E-mail: Trong-On.Do@gch.ulaval.ca.

(1) Downing, E.; Hesselink, L.; Ralston, J.; Macfarlane, T. *Science* **1996**, *273*, 1185–1189.
(2) Gambino, J. R.; Guare, C. J. *Nature* **1963**, *198*, 1084.
(3) Boyer, J. C.; Cuccia, L. A.; Capobianco, J. A. *Nano Lett*. **2007**, *7*, 847–852.
(4) Stouwdam, J. W.; Raudsepp, M.; Veggel, F. V. *Langmuir* **2005**, *21*, 7003–7008.
(5) Matta, J.; Courcot, D.; Abi-Aad, E.; Aboukais, A. *Chem. Mater*. **2002**, *14*, 4118–4125.
(6) Au, C. T.; Zhang, W. D. *J. Chem. Soc., Faraday Trans*. **1997**, *93*, 1195–1204.
(7) Li, K. T.; Chi, Z. H. *Appl. Catal., A* **2001**, *206*, 197–203.
(8) Yan, Z. G.; Yan, C. H. *J. Mater. Chem*. **2008**, *18*, 5046–5059.
(9) Wang, X.; Li, Y. *Chem. Commun*. **2007**, 2901–2910.
(10) Redl, F. X.; Cho, K. S.; Murray, C. B.; O'Brien, S. *Nature* **2003**, *423*, 968–971.
(11) Zarur, A. J.; Ying, J. Y. *Nature* **2000**, *403*, 65–67.
(12) Mrabet, D.; Zahedi-Niaki, M. H.; Do, T. O. *J. Phys. Chem. C* **2008**, *112*, 7124–7129.
(13) Burda, C. B.; Chen, X. B.; Narayanan, R.; Sayed, M. A. E. *Chem. Rev*. **2005**, *105*, 1025–1102.
(14) Liu, J.; Chen, W.; Liu, X.; Zhou, K.; Li, Y. *Nano Res*. **2008**, *1*, 46–55.
(15) Mahapatra, S.; Ramanan, A. *J. Alloys Compd*. **2005**, *395*, 149–153.
(16) Liu, J.; Li, Y. *Mater. Chem*. **2007**, *17*, 1797–1803.
(17) Deng, H.; Yang, S.; Xiao, S.; Gong, H. M.; Wang, Q. Q. *J. Am. Chem. Soc*. **2008**, *130*, 2032–2040.
(18) Deng, H.; Liu, C.; Yang, S.; Xiao, S.; Zhou, Z. K.; Wang, Q. Q. *Cryst. Growth Des*. **2008**, *8*, 4432–4439.
(19) Qian, L.; Zhu, J.; Chen, Z.; Gui, Y.; Gong, Q.; Yuan, Y.; Zai, J.; Qian, X. *Chem.—Eur. J*. **2009**, *15*, 1233–1240.
(20) Luo, F.; Jia, C. J.; Song, W.; You, L. P.; Yan, C. H. *Cryst. Growth Des*. **2005**, *5*, 137–142.
(21) Jia, G.; Song, Y.; Yang, M.; Huang, Y.; Zhang, L.; You, H. *Opt. Mater*. **2009**, *31*, 1032–1037.
(22) Mialon, G.; Gohin, M.; Gacoin, T.; Boilot, J. P. *ACS Nano* **2008**, *2*, 2505–2512.

Scheme 1. Schematic Illustration for the Formation of the $Re(OA)_3$ and $VO_4(TOA)_3$ Complexes (i) and the $ReVO_4$ Nanocrystals (ii)

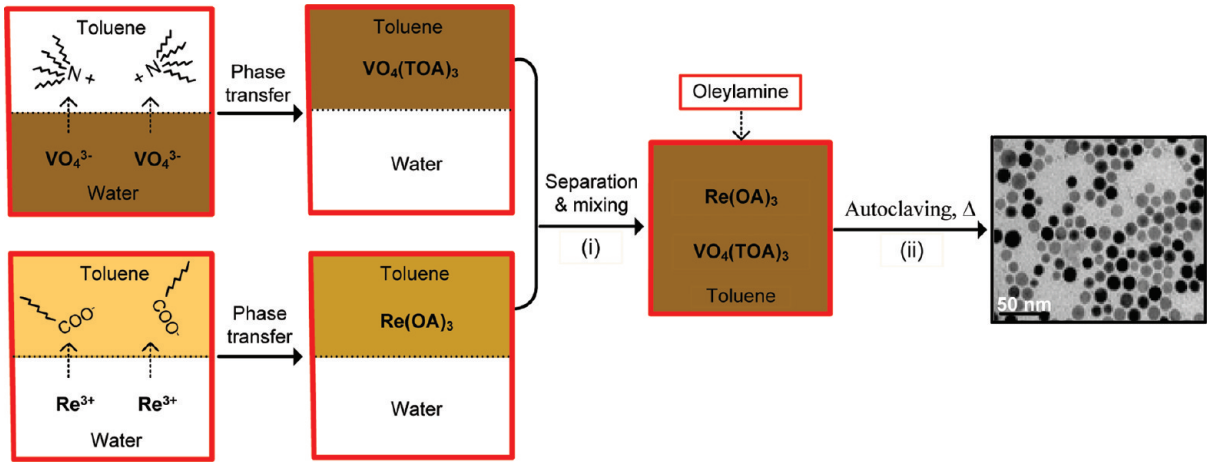

were purchased from Sigma-Aldrich. Sodium hydroxide (NaOH, 97%) and all solvents used such as toluene and ethanol were of analytical grade and purchased from Reagent ACS.

Synthesis of Rare Earth Orthovanadate ($ReVO_4$, Re = Sm and Ce) Nanocrystals. *Preparation of $Re(OA)_3$ Complexes.* To prepare rare earth oleate complexes, an organic solution was produced from adding 40 mL of toluene into the ethanol solution (10 mL) containing potassium oleate (KOA, 6.4 g or 0.008 mol). The organic solution was mixed to 30 mL of a $Re(NO_3)_3 \cdot 6H_2O$ aqueous solution (0.067 mol/L) with a Sm^{3+}/OA^- molar ratio of 1:3 and then transferred to a flask. The two-phase mixtures were heated to 70 °C for 60 min with vigorous stirring, and the organic solution became light yellow after being reacted, indicating the occurrence of the coordinated reaction of Re^{3+} and OA^- for the complex formation. Subsequently, the upper deep orange supernatant toluene solution (40 mL) containing $Re(OA)_3$ complexes (0.059 mol/L) was isolated.

Preparation of $VO_4(TOA)_3$ Complexes. A total of 0.24 g (0.0013 mol) of commercial bulk V_2O_5 powders was dissolved in 20 mL of a 0.12 M NaOH aqueous solution and vigorously stirred at room temperature for 30 min. V_2O_5 powders were completely dissolved in the dilute NaOH solution to give a homogeneous light orange Na_3VO_4 aqueous solution (~0.133 mol/L). Then, 40 mL of toluene solution (0.040 mol/L) containing a cationic phase-transfer reagent ($[CH_3(CH_2)_7]_4NBr$ or TOABr, 0.87 g) was added to the above solution, and the VO_4^{3-}/TOA^+ molar ratio was close to 1:3. The two-phase mixture was vigorously stirred at room temperature. After 30 min, VO_4^{3-} anions in the aqueous phase were completely extracted into the toluene phase, and a light orange toluene solution was observed. Subsequently, the upper light orange supernatant toluene solution (40 mL) containing $VO_4(TOA)_3$ complexes (0.059 mol/L) was isolated.

Synthesis of $ReVO_4$ Nanocrystals. Typically, the two above toluene solution containing $Re(OA)_3$ complexes and $VO_4(TOA)_3$ complexes (0.059 mol/L) were mixed together with a Re/V molar ratio of 1:1, and 0.011 mol (5 mL) of oleylamine (OM) was added under stirring. The reaction solution was transferred into a 120 mL Teflon-lined stainless steel autoclave and was heated at 180 °C for 16 h in an oven. After the reaction, the autoclave was cooled in tap water, and the as-obtained products were easily precipitated by excess ethanol and redispersed preferably in nonpolar solvents (e.g., toluene, hexane, etc.). The precipitation−redispersion process was repeated several times to purify the producing $ReVO_4$ nanocrystals. Different reaction temperatures were tested to control the sizes and the shapes of the $ReVO_4$ nanocrystals. The obtained samples for all of the measurements shown in this communication are directly from synthesis without any size-selection process.

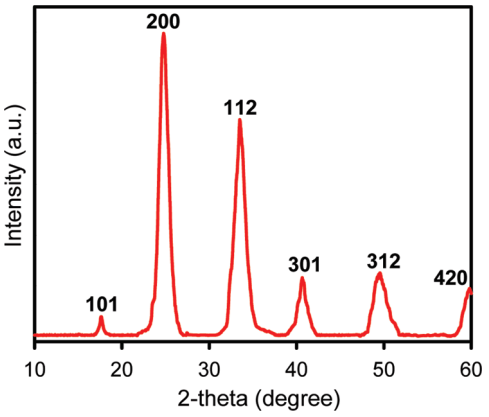

Figure 1. XRD pattern of the as-made $SmVO_4$ nanospheres.

Characterization. The particle sizes and morphologies of the synthesized samarium and cerium orthovanadate nanocrystals were determined at 120 kV by using a JEOL JEM 1230 transmission electron microscope. Samples were prepared by placing a drop of a dilute toluene dispersion of nanocrystals onto a 200 mesh carbon coated copper grid and immediately evaporated at ambient temperature. Particle size distribution diagrams were obtained from statistical treatment of representative TEM images of each sample by measuring the diameter of typically not less than 300 particles using the software ImageJ.[23] Average particle diameters were determined from these size distribution diagrams. The crystalline phases of products were characterized on a Bruker SMART APEXII X-ray diffractometer operated at 1200 W power (40 kV, 30 mA) to generate Cu Kα radiation (λ = 1.5418 Å). The XPS spectra were taken on a photoelectron spectrometer (KRATOS AXIS-ULTRA) with a monochromatic X-ray source of Al Kα. The operating conditions for recording Sm 3d, Ce 3d, V 2p, O 1s, C 1s, and N 1s high-resolution spectra were 1486.6 eV and 225 W, pass energy of 160 eV with an operating pressure of 10^{-9} Torr, acquisition time of 5.75 min, and a pressed mixed oxide pellet under an Ar^+ bombardment. The peaks were deconvoluted by means of standard CasaXPS software (v.2.3.13; product of CasaXPS Software Ltd.) in order to resolve the separate constituents after background subtraction. The UV−vis spectra of the as-synthesized $ReVO_4$ nanocrystals were recorded on a Hitachi U-3010 spectrometer, and pure MgO was used as a blank. The thermal analyses of the as-synthesized

(23) Igathinathane, C.; Pordesimo, L. O.; Batchelor, W. D. *Food Res. Int.* **2009**, *42*, 76–84.Public domain software to be downloaded from http://rsb.info.nih.gov/ij/http://rsb.info.nih.gov/ij/.

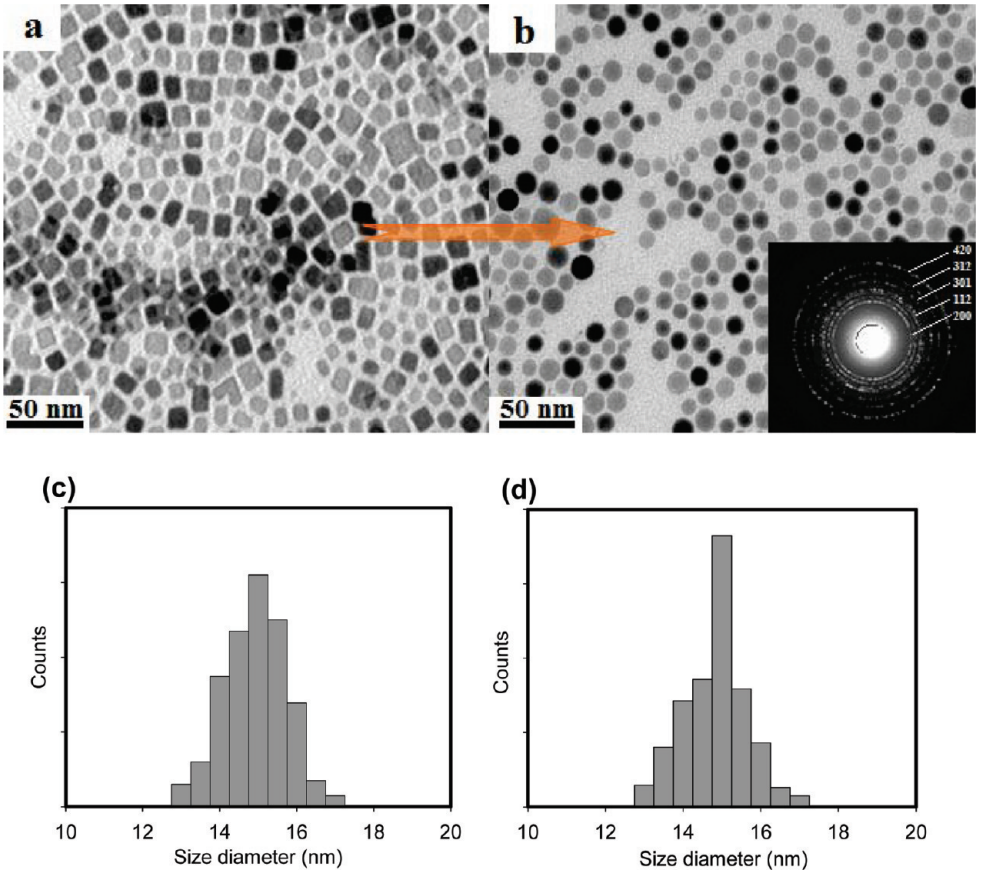

Figure 2. TEM images of 15 nm sized $SmVO_4$ nanocrystals synthesized at different temperatures for 16 h: (a) nanocubes at 150 °C and (c) corresponding particle size distribution; (b) nanospheres at 180 °C (inset, SAED) and (d) corresponding particle size distribution.

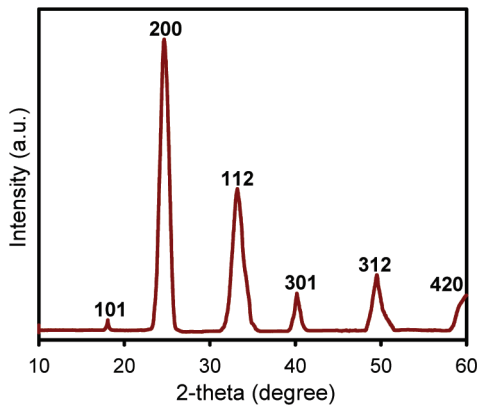

Figure 3. XRD pattern of the as-made $CeVO_4$ nanospheres.

$ReVO_4$ nanocrystals (~5 mg) were carried out at a heating rate of 10 °C/min under an air flux up to 650 °C using a Perkin-Elmer TGA thermogravimetric analyzer. Fourier transform infrared (FTIR) absorption spectra were measured with a FTS 45 infrared spectrophotometer with the KBr pellet technique.

3. Results and Discussion

The synthesis of $ReVO_4$ nanocrystals consists of two steps: (i) the preparation of $Re(OA)_3$ complexes (Re = Sm and Ce) and $VO_4(TOA)_3$ complexes from inexpensive precursors; $Re(NO_3)_3$ and V_2O_5 powders, respectively; (ii) the formation of $ReVO_4$ nanocrystals (e.g., $SmVO_4$ and $CeVO_4$ NCs) from the presynthesized $Re(OA)_3$ and $VO_4(TOA)_3$ complexes. The formation of $ReVO_4$ NCs is schematically illustrated in Scheme 1, and detailed synthesis of these materials is reported in the 2Experimental Section. Metal oxide nanocrystals of Sm_2O_3, CeO_2, and V_2O_5 were also synthesized following the methods reported previously by our group.[24–26]

Figures 1 and 3 show the X-ray diffraction (XRD) patterns of the as-made $SmVO_4$ and $CeVO_4$ nanocrystal samples, respectively. All the XRD peaks are well indexed to tetragonal zircon-type structure with the following lattice contents: $SmVO_4$: $a = b = 7.265$ Å, $c = 6.389$ Å (*Fm*3*hm*, JCPDS card no. 17-0876);[15] $CeVO_4$: $a = b = 7.265$ Å, $c = 6.389$ Å (*I*1/*amd*, JCPDS card no. 12-0757).[17] The intense broadening of the peaks is caused by the small particle sizes. The average crystalline size of these as-made $SmVO_4$ and $CeVO_4$ NC samples calculated from the broadening of the (200) peak using the Scherrer formula are 17.5 and 18.5 nm, respectively. Furthermore, for the corresponding as-made single metal oxide NCs, the XRD patterns exhibit cubic phase (JCPDS card no. 78-0429) for Sm_2O_3,[24] cubic phase (JCPDS card no. 78-0429) for CeO_2,[26] and orthorhombic phase (JCPDS card no. 78-0429) for V_2O_5 (Supporting Information S-Figure 1).[25] Their XRD peaks did not match at all those of the mixed oxide $SmVO_4$ and $CeVO_4$ NCs. Otherwise, no XRD peaks of the $SmVO_4$ and $CeVO_4$ NC samples which correspond to single metal oxide NCs of Sm_2O_3, CeO_2, and V_2O_5 were detected, indicating that the pure tetragonal zircon-type structure of $SmVO_4$ and $CeVO_4$ NCs can be achieved by this method. It can be also concluded that the formation of the pure tetragonal $ReVO_4$ phase results in the

(24) Nguyen, T. D.; Mrabet, D.; Do, T. O. *J. Phys. Chem. C* **2008**, *112*, 15226–15235.
(25) Nguyen, T. D.; Do, T. O. *Langmuir* **2009**, *25*, 5322–5332.
(26) Nguyen, T. D.; Do, T. O. *J. Phys. Chem. C* **2009**, *113*, 11204–11214.

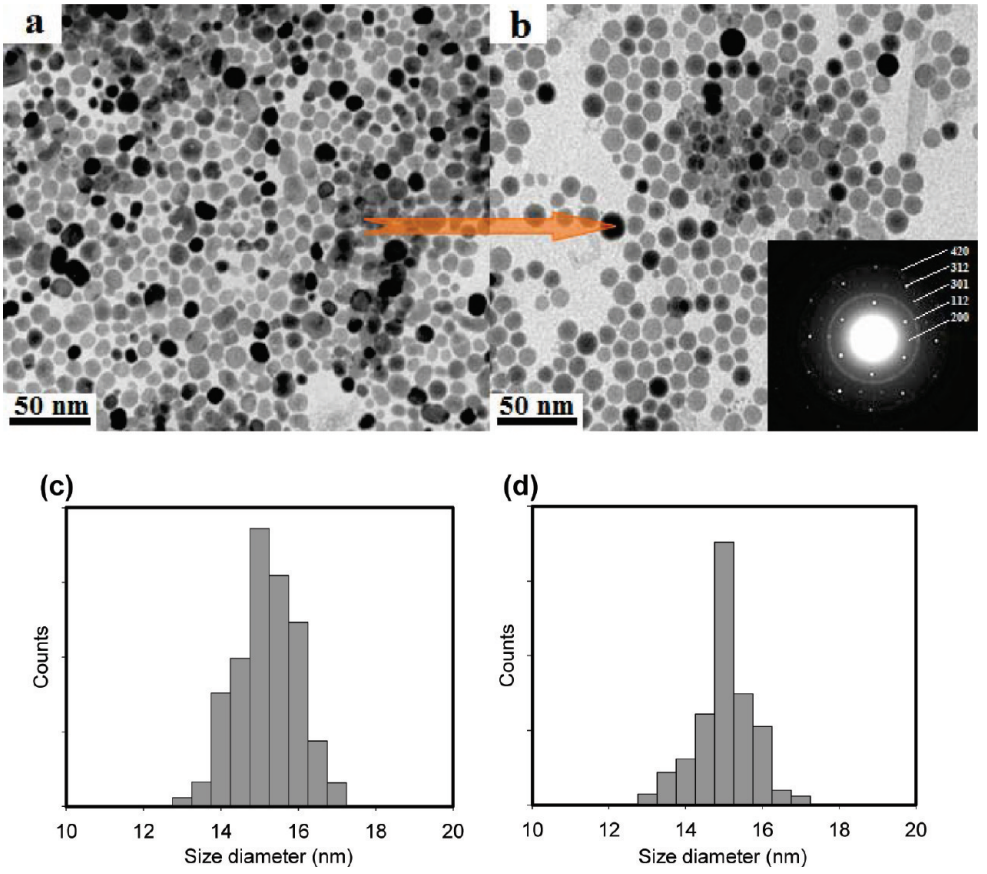

Figure 4. TEM images of 15 nm sized $CeVO_4$ nanocrystals synthesized at different temperatures for 16 h: (a) round-shaped nanocrystals at 150 °C and (c) corresponding particle size distribution; (b) nanospheres at 180 °C (inset, SAED) and (d) corresponding particle size distribution.

complete reaction of the 1:1 ratio of Re^{3+} cation and VO_4^{3-} anion monomers in the bulk solution during the synthesis.

The shape of $SmVO_4$ and $CeVO_4$ NCs could be controlled by the synthesis temperature. TEM images, SEAD patterns, and particle size distribution (PSD) diagrams of the samples synthesized solvothermally at 150 and 180 °C for 16 h are shown in Figures 2 and 4. Nearly cubic-shaped $SmVO_4$ and round-shaped $CeVO_4$ nanocrystals with an average diameter of 15 nm were found at 150 °C. When the synthesis temperature increased to 180 °C for 16 h, both uniform $SmVO_4$ and $CeVO_4$ nanospheres were observed; however, the diameter is unchanged. A slight change in color of the toluene containing nanoparticles from light yellow to brown was observed, when the reaction temperature was increased from 150 to 180 °C, indicating a change in shape of the nanoparticles (Supporting Information S-Figure 3). The inset SAED patterns taken from single particles are also indexed to a tetragonal $SmVO_4$ and $CeVO_4$ single crystal with strong ring patterns from the (200), (112), (301), (312), and (420) planes which are consistent with the XRD results. PSD diagrams of these samples were obtained from the statistical treatment of particle diameters from representative TEM images,[23] as shown in Figures 2c, d and 4c, d. It is found that the PSD becomes narrower, indicating more unifrom nanoparticles, when the reaction temperature is increased from 150 to 180 °C. The transformation of both cubic-shaped $SmVO_4$ and round-shaped $CeVO_4$ NCs into uniform nanospheres while preserving the particle size by increasing synthesis temperature from 150 to 180 °C can be explained by the Wuff facets theory.[27,28] Because no monomer precursors were added during the synthesis, at the relatively low reaction temperature (e.g., 150 °C), the cubic-shaped $SmVO_4$ and round-shaped $CeVO_4$ nanocrystals were formed in the anisotropic growth of high-energy crystal faces owing to high monomer metal concentration in bulk solution.[26] The differences in cubic and round shapes of the $SmVO_4$ and $CeVO_4$ nanocrystals, respectively, could be due to the different nature of their corresponding rare earth metals. At higher synthesis temperature (e.g., 180 °C), the transformation of both the cubic- and round-shaped nanocrystals into uniform nanospheres could result in the depletion of remaining metal monomer concentration in bulk solution to a level lower than that required for a given anisotropic shape.[26] Consequently, the monomers of the dissolved crystals at high energy faces could move to the lower energy faces because of the differences in chemical potential between different crystal faces. As a result, the corners and the tips of the cubic-shaped $SmVO_4$ and round-shaped $CeVO_4$ nanocrystals were "smoothed", which leads to the formation of stable nanospheres with a minimum face energy.

The UV−vis absorption spectra of the as-made $SmVO_4$ and $CeVO_4$ nanosphere samples are shown in Figure 5. A strong absorption peak at 265 and 264 nm for the $SmVO_4$ and $CeVO_4$ samples, respectively, is observed, which is attributed to the charge transfer from the oxygen ligands to the central vanadium

(27) Mullin, J. W. *Crystallization*, 3rd ed.; Butterworth-Heinemann: Woburn, MA, 1997.

(28) Wulff, G.; Zeitschrift, F. *Beitr. Krystallogr. Mineral.* **1901**, *34*, 449.

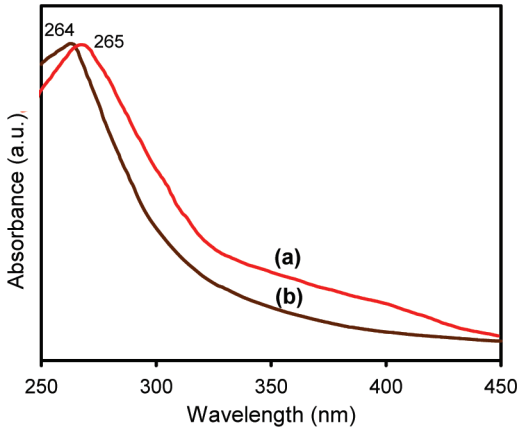

Figure 5. UV−vis absorption spectra of the as-made nanosphere samples: (a) $SmVO_4$ and (b) $CeVO_4$.

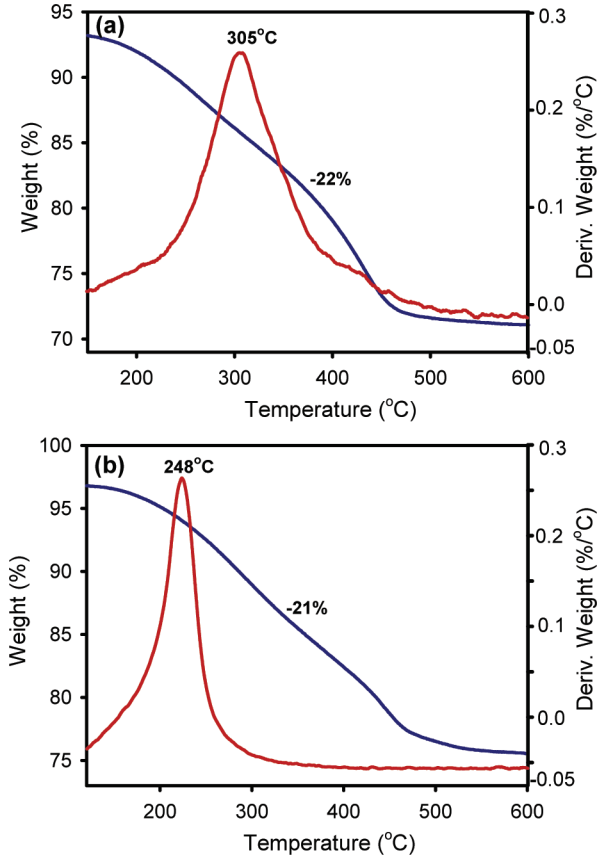

Figure 6. TGA−DTA curves of the OM-capped nanosphere samples: (a) $SmVO_4$ and (b) $CeVO_4$.

atom inside the VO_4^{3-} groups in the samarium and cerium orthovanadate, respectively.[29] However, no significant change in the position of this peak was observed with different shapes of these samples This could be due to almost the same of the nanoparticle size (~15 nm).

The thermogravimetric analysis/differential thermal analysis (TGA−DTA) curves (Figure 6) of the oleylamine (OM)-capped $SmVO_4$ and $CeVO_4$ nanospheres exhibit the weight loss of 22 and 21% appearing around 150−500 °C accompanied by the

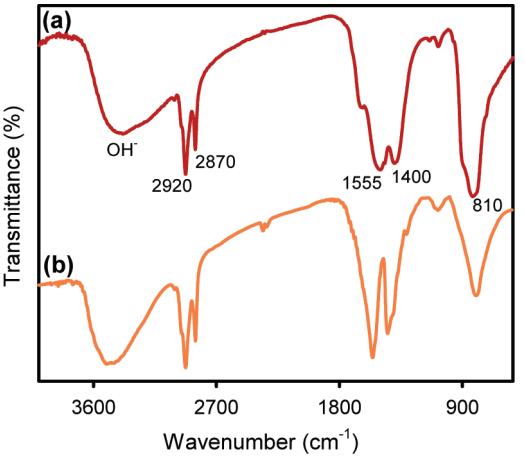

Figure 7. FTIR spectra of the OM-capped nanosphere samples: (a) $SmVO_4$ and (b) $CeVO_4$.

exothermic peaks at 305 and 248 °C, respectively, which are related to the decomposition and combustion of oleylamine molecules on the particle surfaces upon heating. The exothermic peaks of both samples occur at the different two temperatures which can result from the different binding of oleylamine molecules to their corresponding nanocrystal surfaces. The FTIR spectra (Figure 7) of these OM-capped samples show at 2920−2870 cm^{-1} which are assigned to the C−H stretching modes of alkyl chains in oleylamine.[25] The band at 1440 cm^{-1} is attributed to the N−H bending and N−C stretching modes of $-NH_2$ groups in oleylamine capped on nanocrystal surfaces.[25] The IR band at 810 cm^{-1} is attributed to the Re−O−V vibrations of $ReVO_4$.[30] Residual water and a hydroxide group are detected with a large band around 3450 cm^{-1}, corresponding to the O−H stretching frequency due to the bending vibration of associated water. These data suggest that oleylamine molecules were bound to the nanocrystal surface and further confirm that $SmVO_4$ and $CeVO_4$ were formed under these synthetic conditions.

The metal oxidation states on the particle surface of the $SmVO_4$ and $CeVO_4$ NCs and corresponding single metal oxides (e.g., Sm_2O_3, CeO_2, V_2O_5) were examined by XPS. The survey XPS spectra of these as-made and calcined mixed oxide NC samples in a wide energy range are presented in S-Figures 3 and 4 in the Supporting Information; beside carbons and nitrogens, no impurities were found. However, the intense C 1s and N 1s peaks of the as-made samples as compared to those of the calcined samples can be assigned to the oleylamine ligand capped on the NC surface. The positions of XPS peaks were corrected using the C 1s core level taken at 285 eV as a binding energy (BE) reference. Surprisingly, the Sm 3d, Ce 3d, and V 2p XPS spectra of both the as-made and calcined $SmVO_4$ and $CeVO_4$ nanospheres exhibit only one oxidation state for each metal (e.g., Sm^{3+}, Ce^{3+}, V^{5+}) at the nanoscale and even in ultrahigh vacuum for XPS measurements (see Figures 8 and 9). The Sm $3d_{5/2,3/2}$ peaks at 1083.5−1110.8 eV, the Ce $3d_{5/2,3/2}$ peaks at 885.7−904.0 eV, and the V $2p_{3/2,1/2}$ peaks at 517.2−525.5 eV attributed to Sm^{3+}, Ce^{3+}, and V^{5+}, respectively, were observed.[24,31] No peaks characteristic of other metal oxidation states of these metals were detected. However, for the single NC samples of samaria, ceria, vanadia, the Sm 3d, Ce 3d, and V 2p XPS spectra exhibit two additional weak peaks at 1095.9−1121.3 eV for Sm^{2+} $3d_{5/2,3/2}$,

(29) Kalai Selvan, R.; Gedanken, A.; Anilkumar, P.; Manikandan, G.; Karunakaran, C. *J. Cluster Sci.* **2008**, DOI: 10.1007/s10876-008-0229-y.

(30) Fang, Z. M.; Hong, Q.; Zhou, Z. H.; Dai, S. J.; Weng, W. Z.; Wan, H. L. *Catal. Lett.* **1999**, *61*, 39–44.

(31) Salvi, A. M.; Decker, F.; Varsano, F.; Speranza, G. *Surf. Interface Anal.* **2001**, *31*, 255–264.

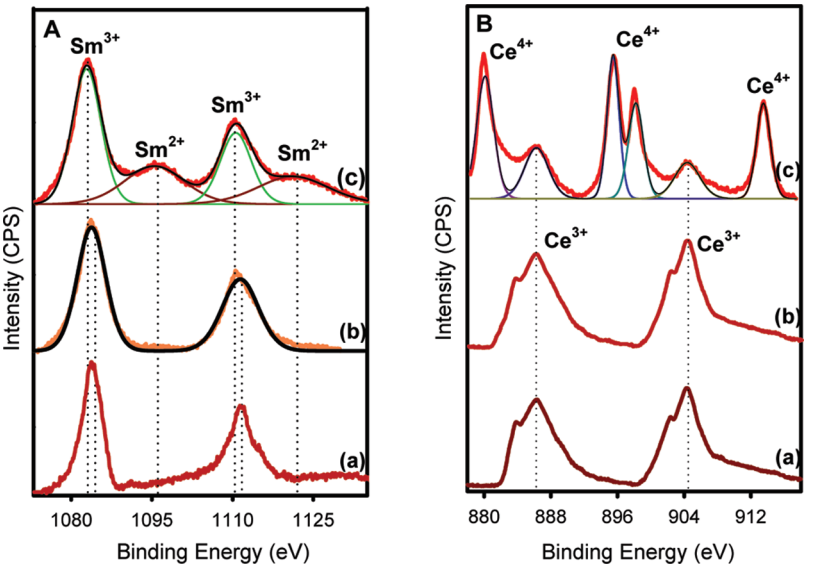

Figure 8. (A) Sm 3d XPS spectra of (a) the as-made SmVO4 nanospheres, (b) the calcined $SmVO_4$ nanospheres, and (c) the calcined Sm_2O_3 nanospheres. (B) Ce 3d XPS spectra of (a) the as-made $CeVO_4$ nanospheres, (b) the calcined $CeVO_4$ nanospheres, and (c) the calcined CeO_2 nanospheres.

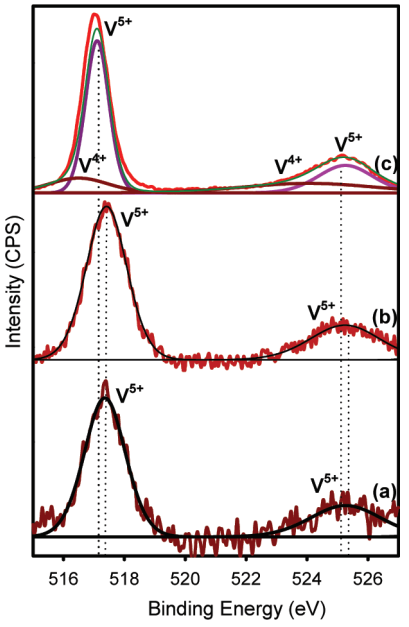

Figure 9. V 2p XPS spectra of the spherical NC samples: (a) as-made $SmVO_4$ NCs, (b) calcined $SmVO_4$ NCs, and (c) calcined V_2O_5 NCs.

at 879.5−914.0 eV for Ce^{3+} $3d_{5/2,3/2}$, and at 516.2−524.1 eV for V^{4+} $2p_{5/2,3/2}$, as compared to those of the mixed oxide $SmVO_4$ and $CeVO_4$ nanosphere samples. It means that, in these single metal oxide NC samples, these metals exist in two oxidation states, and the fit peaks revealed Sm^{3+} (60%) and Sm^{2+} (40%) for samarium,[24] Ce^{4+} (54%) and Ce^{3+} (46%) for cerium,[26] V^{5+} (65%) and V^{4+} (35%) for vanadium.[25]

The XPS results revealed that, for each metal, only one oxidation state (e.g., Sm^{3+}, Ce^{3+}, V^{5+}) exhibits in the $SmVO_4$ and $CeVO_4$ NCs, and meanwhile, two oxidation states (Sm^{3+}/Sm^{2+}, Ce^{4+}/Ce^{3+}, V^{5+}/V^{4+}) in the single Sm_2O_3, CeO_2, V_2O_5 NCs were found. This difference is due to the fact that, for each single metal oxide, the single Sm−O−Sm bonds in Sm_2O_3, the Ce−O−Ce bonds in CeO_2, and the V−O−V bonds in V_2O_5 allow the multiple oxidation states, whereas, for the mixed metal oxides, the presence of mixed Sm−O−V bonds in $SmVO_4$ and Ce−O−V bonds in $CeVO_4$ requires the formation of Sm^{3+}−V^{5+} and Ce^{3+}−V^{5+} species, respectively.[5,32,33] In fact, the formation of the $ReVO_4$ phase (Re = Sm and Ce) results in the interaction between the nuclear spin of the V atom and unpaired 4f electron of Re. Fermi contact interaction could be involved with a transfer of the unpaired 4f electron of the Re ions to the orbital on the V atom,[34−36] and hence a slight chemical shift to a higher binding energy (shifted ∼0.3−1.3 eV) of Sm 3d, Ce 3d, and V 2p of $ReVO_4$ NCs compared with that of Sm_2O_3, CeO_2, and V_2O_5 NCs.[5,37] As a result, V and Re possess a valence of +5 and +3, respectively, in the $ReVO_4$ lattice.

For the $CeVO_4$ NCs, as seen in Figure 10a, the O 1s peak at 530.2 eV is attributed to both O−Re and O−V bonds in the tetragonal $ReVO_4$ lattice[31] which consists of VO_4 tetrahedra which share corners and edges with ReO_8 dodecahedra,[15,17] and another shoulder peak at 532.2−533.1 eV is attributed to the presence of hydroxyl species or adsorbed water on the nanocrystal surface.[24] However, for the $SmVO_4$ NCs (Figure 10b), the XPS peak at ∼530 eV is broader with a full width at half-maximum (fwhm = 2.0 eV) as compared to the O 1s peak (fwhm = 1.0 eV) for the $CeVO_4$ NCs. The broader peak at ∼530 eV could be associated with a Sm Auger peak (∼526.8 eV).[38,39] The XPS analysis confirms that the molar ratio of Re/V in these samples is very close to 1:1, agreeing with the formula of $ReVO_4$. It is well-known that stoichiometric defects such as oxygen vacancies and

(32) Shah, P. R.; Khader, M. M.; Vohs, J. M.; Gorte, R. J. *J. Phys. Chem. C* **2008**, *112*, 2613–2617.
(33) Shah, P. R.; Vohs, J. M.; Gorte, R. J. *J. Phys. Chem. B* **2007**, *111*, 5680–5683.
(34) Reidy, R. F.; Swider, K. E. *J. Am. Ceram. Soc.* **1995**, *78*, 1121–1122.
(35) Cousin, R.; Dourdin, M.; Abi-Aad, E.; Courcot, D.; Capelle, S.; Guelton, M.; Aboukaís, A. *J. Chem. Soc., Faraday Trans.* **1997**, *93*, 3863–3867.
(36) Cousin, R.; Courcot, D.; Abi-Aad, E.; Capelle, S.; Amoureux, J. P.; Dourdin, M.; Guelton, M.; Aboukaís, A. *Colloids Surf., A* **1999**, *158*, 43–49.
(37) Beche, E.; Charvin, P.; Perarnau, D.; Abanades, S.; Flamant, G. *Surf. Interface Anal.* **2008**, *40*, 264–267.
(38) Moulder, J. F.; Stickle, W. F.; Sobol, P. E.; Bomben, K. D. *Handbook of X-ray photoelectron spectroscopy*; Perkin-Elmer corporation, Physical Electronics Division: 1992.
(39) Turner, N. H.; Schreifels, J. A. *Anal. Chem.* **1996**, *68*, 309–332.

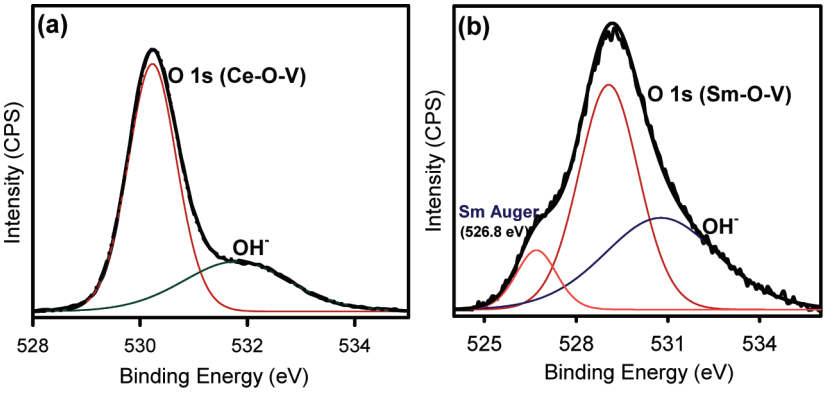

Figure 10. O 1s XPS spectra of the as-made spherical mixed oxide samples: (a) $CeVO_4$ NCs and (b) $SmVO_4$ NCs.

their mobility on the metal oxide surface at reaction temperature are of great importance for redox reactions.[35,40,41] Further work to determine the amount of oxygen released of both lattice oxygen and adsorbed oxygen species from these mixed oxide NCs using the TPD-O_2 technique as well as the nature of oxygen species involved in catalytic oxidation is in progress in our laboratory.

4. Conclusions

We have developed a simple and reproducible method for the synthesis of uniform $SmVO_4$ and $CeVO_4$ nanocrystals from the solvolysis of a mixture of $Re(OA)_3$ (Re = Sm and Ce) and $VO_4(TOA)_3$ complexes in toluene in the presence of oleylamine ligand. By increasing the reaction temperature from 150 to 180 °C, $SmVO_4$ and $CeVO_4$ NCs can converted from cubic-shaped $SmVO_4$ and nearly round-shaped $CeVO_4$ to uniform nanospheres. The XPS results revealed that only one oxidation state of samarium, cerium, and vanadium for each metal (e.g., Sm^{3+}, Ce^{3+}, V^{5+}) exists in the mixed oxide spherical NCs, $SmVO_4$ and $CeVO_4$, while two oxidation states for each metal (Sm^{3+}/Sm^{2+}, Ce^{4+}/Ce^{3+}, V^{5+}/V^{4+}) exist in the corresponding single metal oxide spherical NCs, Sm_2O_3, CeO_2, and V_2O_5. Our synthetic approach could also be useful for the synthesis of other uniform rare earth orthovanadate, molybdate, and tungstate nanocrystals as well as doped NCs and multicomponent NCs.

Acknowledgment. This work was supported by the Natural Sciences and Engineering Research Council of Canada (NSERC) through a strategic grant.

Supporting Information Available: XRD patterns, TEM images, corresponding SAED patterns, and survery XPS spectra. This material is available free of charge via the Internet at http://pubs.acs.org.

(40) Do, T. O.; Nguyen, S. V.; Kaliaguine, S. *Phys. Chem. Chem. Phys.* **2003**, *5*, 2724–2729.
(41) Levasseur, B.; Kaliaguine, S. *J. Solid State Chem.* **2008**, *181*, 2953–2963.

Monodisperse Samarium and Cerium Orthovanadate Nanocrystals and Metal Oxidation States on the Nanocrystal Surface

Thanh-Dinh Nguyen, Cao-Thang Dinh, and Trong-On Do*

Department of Chemical Engineering, Laval University, Quebec G1K 7P4 Canada

To whom correspondence should be addressed. E-mail: Trong-On.Do@gch.ulaval.ca

SUBMITTED TO *Langmuir* – April 2009

Supporting Information

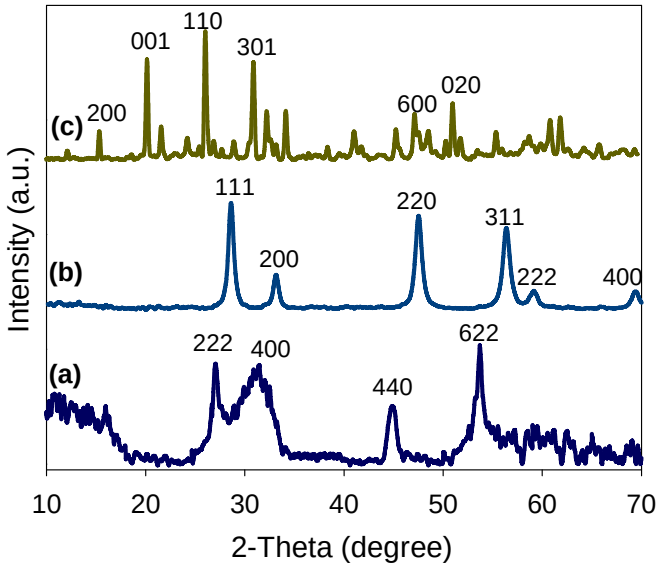

S-Figure 1. XRD patterns of the calcined single metal oxide spherical NCs: (a) Sm_2O_3, (b) CeO_2, (c) V_2O_5.

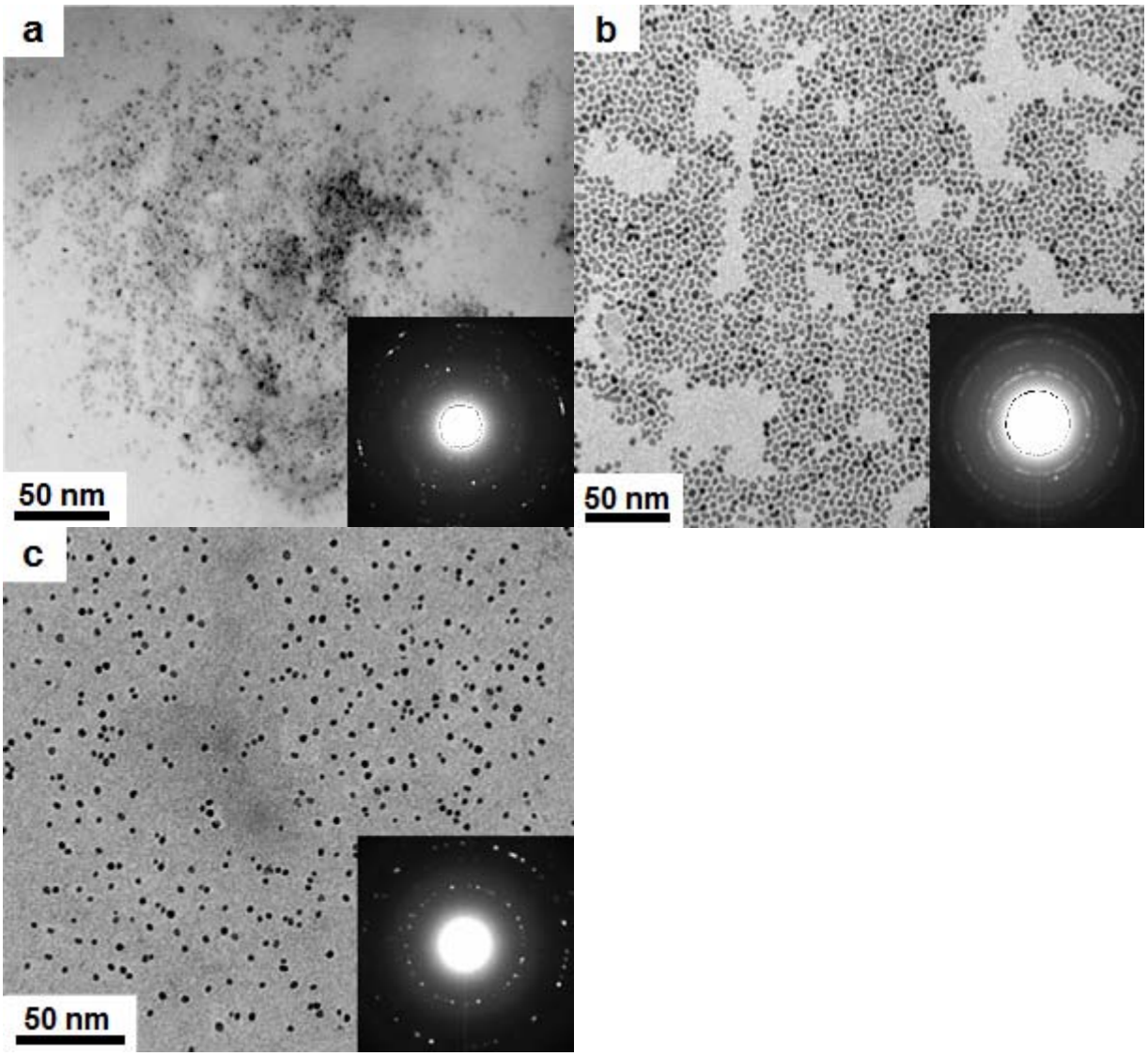

S-Figure 2. TEM images and corresponding inset SAED patterns of the as-made single metal oxide spherical NCs: (a) Sm_2O_3, (b) CeO_2, (c) V_2O_5.

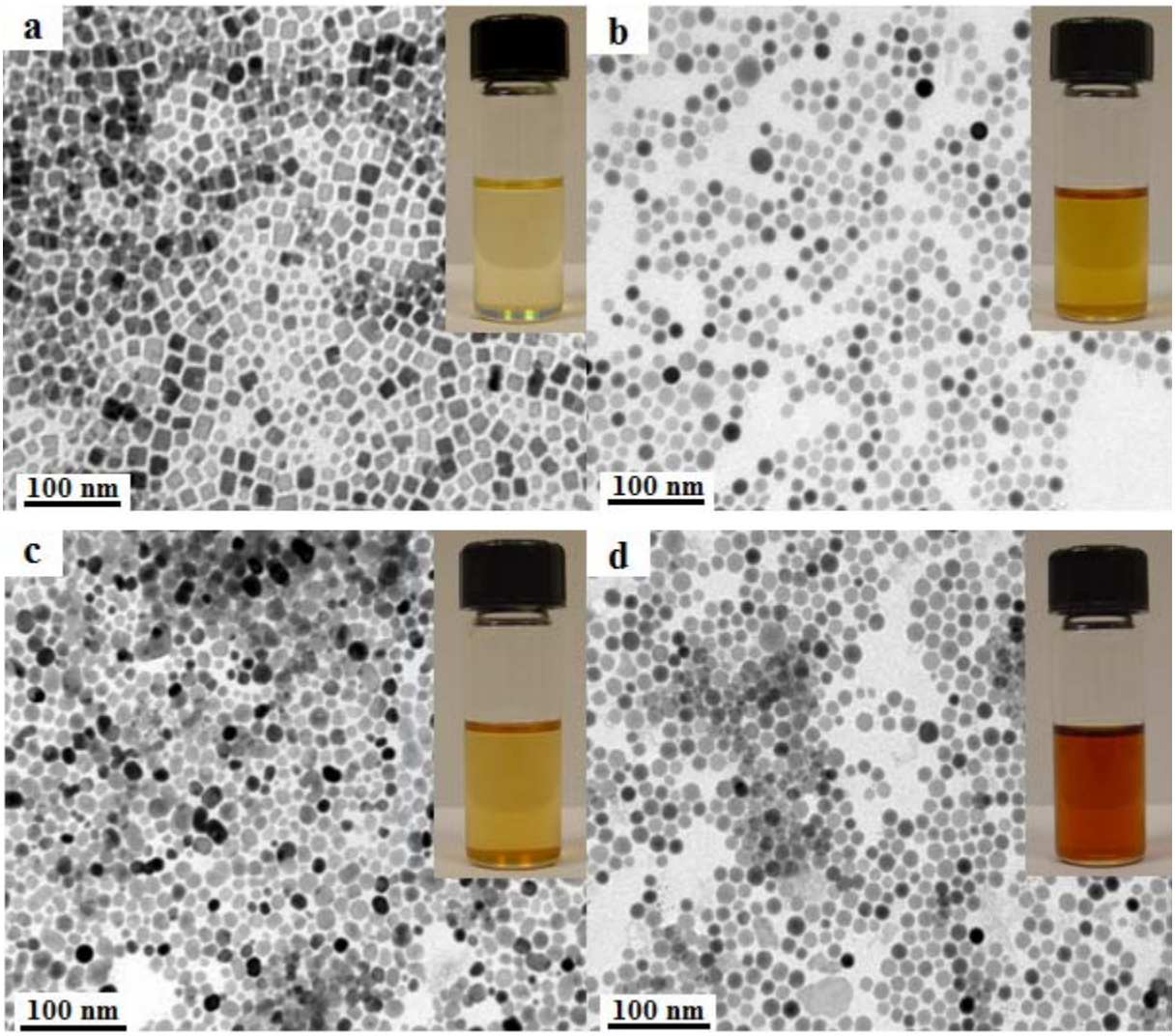

S-Figure 3. TEM images of the 15 nm $ReVO_4$ nanocrystal samples and color photographes of the transparent toluene solution containing oleylamine-capped nanocrystals synthesized solvothermally at different temperatures for 16 h:

- $SmVO_4$: (a) nanocubes at 150 ^oC, (b) nanospheres at 180 ^oC, and their corresponding photograph (inset).

- $CeVO_4$: (c) round-shaped nanocrystals at 150 ^oC, (d) nanospheres at 180 ^oC, and their corresponding photograph (inset).

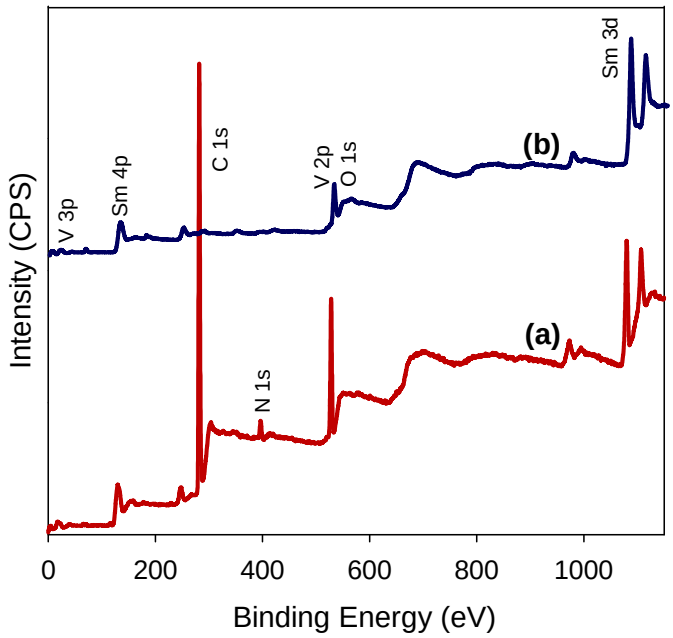

S-Figure 4. Survey XPS spectra of the as-made $SmVO_4$ nanospheres obtained before (a) and after (b) calcination at 550 ^{o}C for 2 h.

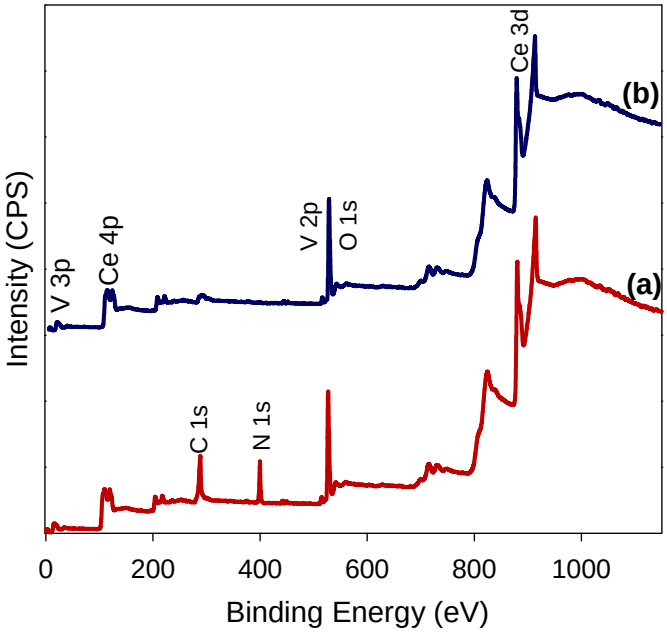

S-Figure 5. Survey XPS spectra of the as-made $CeVO_4$ nanospheres obtained before (a) and after (b) calcination at 550 ^{o}C for 2 h.